Available online at www.sciencedirect.com
ScienceDirect
Advances in Water Resources 30 (2007) 1342–1354
Advances in Water Resources
www.elsevier.com/locate/advwatres

Effective dispersion in a chemically heterogeneous medium under temporally fluctuating flow conditions

Vanessa Zavala-Sanchez, Marco Dentz *, Xavier Sanchez-Vila

Department of Geotechnical Engineering and Geosciences, Technical University of Catalonia (UPC), Barcelona, Spain

Received 10 August 2006; received in revised form 23 November 2006; accepted 27 November 2006
Available online 17 January 2007

Abstract

We investigate effective solute transport in a chemically heterogeneous medium subject to temporal fluctuations of the flow conditions. Focusing on spatial variations in the equilibrium adsorption properties, the corresponding fluctuating retardation factor is modeled as a stationary random space function. The temporal variability of the flow is represented by a stationary temporal random process. Solute spreading is quantified by effective dispersion coefficients, which are derived from the ensemble average of the second centered moments of the normalized solute distribution in a single disorder realization. Using first-order expansions in the variances of the respective random fields, we derive explicit compact expressions for the time behavior of the disorder induced contributions to the effective dispersion coefficients. Focusing on the contributions due to chemical heterogeneity and temporal fluctuations, we find enhanced transverse spreading characterized by a transverse effective dispersion coefficient that, in contrast to transport in steady flow fields, evolves to a disorder-induced macroscopic value (i.e., independent of local dispersion). At the same time, the asymptotic longitudinal dispersion coefficient can decrease. Under certain conditions the contribution to the longitudinal effective dispersion coefficient shows superdiffusive behavior, similar to that observed for transport in s stratified porous medium, before it decreases to its asymptotic value. The presented compact and easy to use expressions for the longitudinal and transverse effective dispersion coefficients can be used for the quantification of effective spreading and mixing in the context of the groundwater remediation based on hydraulic manipulation and for the effective modeling of reactive transport in heterogeneous media in general.

Keywords: Reactive transport; Transverse dispersion; Temporal random flow; Random adsorption; Stochastic modeling; Effective dispersion

1. Introduction

The quantitative and qualitative understanding of transport in heterogeneous hydrogeochemical systems is of critical importance for transport modeling in natural groundwater systems, and as such a precondition for the analysis of groundwater contamination problems and for the design of soil and aquifer remediation strategies.

Local scale physical and chemical medium heterogeneities lead to an effective large scale transport behavior that is qualitatively and quantitatively different from the one observed in homogeneous media. The interaction of spatial fluctuations of the system parameters and local scale transport processes leads in general to enhanced solute spreading and mixing. The influence of spatially fluctuating physical and chemical system properties, such as hydraulic conductivity and sorption properties, for example, on solute transport has been studied extensively during the last two decades within the stochastic perturbative approach e.g. [1–6], among others. The later studies disregard the effects of local dispersion or focus on the asymptotic long time behavior of solute transport. The full temporal evolution of effective solute spreading in a chemically and physically heterogeneous medium for finite local dispersion has been studied in terms of the time behavior of effective

* Corresponding author.
E-mail addresses: vanessa.zavala@upc.edu (V. Zavala-Sanchez), marco.dentz@upc.edu (M. Dentz), xavier.sanchez-vila@upc.edu (X. Sanchez-Vila).

0309-1708/$ - see front matter © 2006 Elsevier Ltd. All rights reserved.
doi:10.1016/j.advwatres.2006.11.010

dispersion coefficients, see e.g. [7–9]. The stochastic perturbative analysis yields an increase of the longitudinal effective dispersion coefficient to a macroscopic value as a result of physical and chemical medium heterogeneities, which is in agreement with experimental and numerical findings. The predicted asymptotic transverse dispersion coefficients, however, consistently underestimate numerical and experimental observations by at least one order of magnitude e.g. [10–12]. Recently, the scale dependence of macrodispersion and effective retardation factors for reactive chemicals have been studied in laboratory scale experiments [13] and critically compared to stochastic theories [14]. Lichtner and Tartakovsky [15] studied upscaled effective rate constants for heterogeneous reactions and their evolution with time, which are intimately connected to the observed scale dependence.

Transverse mixing is an important process for geochemical processes in rivers [16], stream–aquifer interactions [17], saltwater intrusion [18,19], and microbial reactions [20,21]. The importance of transverse mixing for reactive transport modeling including precipitation (dissolution) reactions has recently been shown by [22]. As such, the correct quantification of transverse mixing and spreading is significant for the assessment of remediation schemes that rely on the efficient mixing of a reactant with the solved contaminant.

In addition to spatial fluctuations of the system parameters due to physical and chemical medium heterogeneities, groundwater flow in general also fluctuates temporally on a range of scales including hyper annual climatic fluctuations, seasonal and irrigation cycles and daily barometric fluctuations, for example. Such temporal flow fluctuations were first recognized as a source of enhanced solute spreading by Kinzelbach and Ackerer [23]. Rehfeldt and Gelhar [24] presented a stochastic approach for the quantification of the impact of temporal flow fluctuations in a physically heterogeneous medium. Within such a stochastic framework, Kabala and Sposito [25] studied macrodispersion for reactive transport in a spatially heterogeneous medium. Solute spreading in a heterogeneous medium for periodic (deterministic) time fluctuations of the hydraulic gradient for purely advective transport (vanishing local dispersion) has been analyzed by, e.g., Zhang and Neuman [26] and Dagan et al. [27]. Recently, Cirpka [28] studied the enhancement of transverse dispersion of kinetically sorbing compounds in spatially uniform flow field under sinusoidal (deterministic) temporal fluctuations and vanishing local dispersion.

A recent approach to characterize and quantify effective spreading and mixing in time-fluctuating flow through a physically heterogeneous medium is an analysis in terms of effective dispersion coefficients [29–31]. Effective dispersion coefficients characterize effective solute spreading and mixing in an heterogeneous environment [7,8,32]. For transport in time fluctuating spatial random flow fields, it was shown that the interaction between temporal fluctuations, local dispersion and spatial heterogeneity leads to macroscopic contributions to the longitudinal as well as, and more importantly, the transverse effective dispersion coefficients [29–31].

Here we study the impact of the interaction of local dispersion, chemical heterogeneity and temporal fluctuations of the flow conditions on the effective transport behavior of a sorbing solute. We focus on linear sorption reactions under instantaneous local equilibrium conditions. In a chemical heterogeneous medium, the local sorption properties are subject to spatial fluctuations, which can be characterized by a spatially varying retardation coefficient. The effective transport behavior in this practically relevant scenario is studied within a stochastic perturbative approach. Within this approach we derive compact analytical expressions for the temporal evolution of the longitudinal and transverse effective dispersion coefficients.

2. Basics

The objective is to quantify effective solute spreading and mixing of a sorbing chemical in terms of effective transport coefficients. To this end, in the following we define the observables that characterize solute spreading and mixing. We present the stochastic model used, and lay out the perturbation method to solve the resulting stochastic transport problem.

2.1. Observables

The total concentration distribution of the sorbing chemical is divided into a mobile fraction that is transported in the flow through the medium, and a fraction that is adsorbed to the solid matrix,

$$c(\mathbf{x},t) = \phi(\mathbf{x})c_{\mathrm{m}}(\mathbf{x},t) + [1-\phi(\mathbf{x})]c_{\mathrm{ad}}(\mathbf{x},t), \tag{1}$$

where $c_{\mathrm{m}}(x,t)$, and $c_{\mathrm{ad}}(x,t)$ denote the spatial distributions of the mobile and adsorbed concentrations, respectively; and $\phi(x)$ denotes porosity.

As the simplest measures for the analysis of the evolution of the sorbing chemical, we study the effective center of mass velocity and effective dispersion coefficients of the (normalized) distribution density of mobile solute fraction [7],

$$p(\mathbf{x},t) = \frac{c_{\mathrm{m}}(\mathbf{x},t)}{\int \mathrm{d}^d y c_{\mathrm{m}}(\mathbf{y},t)}. \tag{2}$$

In a given aquifer the center of mass velocity and dispersion coefficients are defined by

$$u_j(t) = \frac{\mathrm{d}}{\mathrm{d}t} m_j^{(1)}(t), \tag{3}$$

$$D_{ij}(t) = \frac{1}{2}\frac{\mathrm{d}}{\mathrm{d}t}[m_{ij}(t)^{(2)} - m_i^{(1)}(t)m_j^{(1)}(t)], \tag{4}$$

where $m_i^{(1)}(t)$ and $m_{ij}^{(2)}(t)$ are the first and second moments of the normalized spatial concentration distribution, defined as

$$m_i^{(1)}(t) = \int \mathrm{d}^d x x_i p(\mathbf{x},t), \tag{5}$$

$$m_{ij}^{(2)}(t) = \int \mathrm{d}^d x x_i x_j p(\mathbf{x},t). \tag{6}$$

As detailed in Section 2.3, in a stochastic analysis, the spatially heterogeneous aquifer is identified with one particular realization of an ensemble of aquifer realizations, while the temporally fluctuating groundwater flow is modeled by a correlated stationary random process. In such an approach, the effective transport coefficients can be expressed as averages over the ensemble of all possible realizations of the spatial and temporal random processes. The effective transport velocity and dispersion coefficients are then defined as the ensemble averages over their local scale counterparts (3) and (4), respectively, [29,31],

$$u_i^{\mathrm{eff}}(t) = \langle \overline{u_j(t)} \rangle = \frac{\mathrm{d}}{\mathrm{d}t} \langle \overline{m_j^{(1)}(t)} \rangle, \tag{7}$$

$$D_{ij}^{\mathrm{eff}}(t) = \langle \overline{D_{ij}(t)} \rangle = \frac{1}{2} \frac{\mathrm{d}}{\mathrm{d}t} [\langle \overline{m_{ij}^{(2)}(t) - m_i^{(1)}(t) m_j^{(1)}(t)} \rangle], \tag{8}$$

where the overbar denotes the average over the spatial random field, the angular brackets denote the average over the temporal random process. The effective dispersion coefficient characterizes physical spreading and mixing in a typical disorder realization (e.g. [7,32]), as opposed to the frequently considered ensemble dispersion coefficients, which are derived from the ensemble averaged concentration distribution. The effective dispersion coefficient for finite local dispersion has been analyzed by [7–9] for transport in a physically and chemically heterogeneous medium under steady flow conditions, and [29–31] for passive transport in temporally fluctuating flow. The relevance of effective dispersion coefficients for the quantification of solute mixing and thus for reactive transport modeling has been outlined by [33–35]. Thus, here we focus exclusively on the analysis of the effective transport velocity and dispersion coefficients.

2.2. Transport model

The temporal evolution of the mobile concentration $c_{\mathrm{m}}(\mathbf{x},t)$ under spatially varying equilibrium sorption properties can be described by (e.g. [7]),

$$R(\mathbf{x}) \frac{\partial c_{\mathrm{m}}(\mathbf{x},t)}{\partial t} + \mathbf{q}(\mathbf{x},t) \cdot \nabla c_{\mathrm{m}}(\mathbf{x},t) - \nabla \mathbf{D}_0 \nabla c_{\mathrm{m}}(\mathbf{x},t) = \rho(\mathbf{x}) \delta(t), \tag{9}$$

where the retardation coefficient is defined by [7],

$$R(\mathbf{x}) \equiv \phi(\mathbf{x}) + [1 - \phi(\mathbf{x})] k_{\mathrm{d}}(\mathbf{x}), \tag{10}$$

with a positive spatially varying distribution coefficient $k_{\mathrm{d}}(\boldsymbol{x})$. Note that for technical convenience $t \in (-\infty, +\infty)$, see e.g. [7].

The (constant) local dispersion tensor D_0 is assumed to be diagonal, i.e., $D_{ij} = \delta_{ij} D_{ij}$; $\mathbf{q}(\mathbf{x},t)$ is the divergence-free spatio-temporally fluctuating Darcy velocity (e.g. [24,29]).

The right side of (9) represents the initial condition for an instantaneous solute injection at $t = 0$, $c_{\mathrm{m}}(\mathbf{x}, t = 0) = \rho(\mathbf{x})$. This implies for the mobile concentration $c_{\mathrm{m}}(\mathbf{x}, t = 0) = R(\mathbf{x})^{-1} \rho(\mathbf{x})$.

Here we study transport for a solute evolving from a point-like injection at $t = 0$, i.e., $\rho(\mathbf{x}) = \delta(\mathbf{x})$. We assume vanishing concentration at the boundaries at infinity.

2.3. Stochastic model

The spatially fluctuating retardation factor $R(\mathbf{x})$ and the hydraulic conductivity $K(\mathbf{x})$ here are modeled as stationary spatial random fields, while the temporal fluctuations of the flow boundary conditions that induce a fluctuating mean hydraulic gradient are modeled as a stationary temporal random process (e.g. [24,29])

We split the retardation factor into its mean value and fluctuations about it

$$R(\mathbf{x}) = \overline{R}[1 - \mu(\mathbf{x})], \tag{11}$$

where $\overline{R}$ is the ensemble averaged retardation factor, $\mu(\mathbf{x})$ denotes the normalized fluctuation, whose ensemble average is zero by definition, $\overline{\mu(\mathbf{x})} = 0$. The correlation function of the normalized retardation fluctuations is given by

$$\overline{\mu(\mathbf{x}) \mu(\mathbf{x}')} = \sigma_{\mu\mu}^2 C^{\mu\mu}(\mathbf{x} - \mathbf{x}'), \tag{12}$$

where the variance $\sigma_{\mu\mu}^2 = \overline{\mu(\mathbf{x})^2}$. The correlation function $C^{\mu\mu}$ is assumed to decay exponentially fast for distances larger than the correlation length l.

Rescaling the mobile concentration and the flow velocity as well as the local dispersion coefficients by mean retardation according to,

$$g(\mathbf{x},t) = \overline{R} c_{\mathrm{m}}(\mathbf{x},t), \quad \mathbf{D} = \frac{\mathbf{D}_0}{\overline{R}}, \quad \mathbf{u}(\mathbf{x},t) = \frac{\mathbf{q}(\mathbf{x},t)}{\overline{R}}, \tag{13}$$

we obtain from (9) a transport equation for $g(\mathbf{x},t)$,

$$\frac{\partial g(\mathbf{x},t)}{\partial t} + \mathbf{u}(\mathbf{x},t) \cdot \nabla g(\mathbf{x},t) - \nabla \cdot \mathbf{D} \nabla g(\mathbf{x},t) = \delta(\mathbf{x}) \delta(t) + \mu(\mathbf{x}) \frac{\partial g(\mathbf{x},t)}{\partial t}. \tag{14}$$

Note that the normalized mobile concentration (2) reads in terms of the rescaled mobile concentration $g(\mathbf{x},t)$ as,

$$p(\mathbf{x},t) = \frac{g(\mathbf{x},t)}{\int \mathrm{d}^d y g(\mathbf{y},t)}. \tag{15}$$

For quasi-steady flow conditions, i.e., instantaneous propagation of a temporal change in the flow boundary conditions, the normalized first-order solution of the flow problem (in the fluctuations of the log-hydraulic conductivity) can be decomposed as (e.g. [24,29])

$$\mathbf{u}(\mathbf{x},t) = \mathbf{u}(t) - \mathbf{u}'(\mathbf{x},t). \tag{16}$$

The mean flow direction is aligned with the 1-direction of the coordinate system

$$\langle \overline{\mathbf{u}(\mathbf{x},t)} \rangle = u \mathbf{e}_1 \tag{17}$$

with $\mathbf{e}_1$ the unit vector in 1-direction. The purely time-dependent part is given by

$$\mathbf{u}(t) = u[\mathbf{e}_1 - \boldsymbol{v}(t)] \tag{18}$$

with the normalized purely temporal velocity fluctuations $\boldsymbol{v}(t)$, whose mean is zero by definition,

$$\langle \boldsymbol{v}(t) \rangle = \langle \overline{\mathbf{u}'(\mathbf{x},t)} \rangle \equiv 0. \tag{19}$$

A brief discussion of the quality of the approximation of quasi-steady flow is given in [31]. The correlation functions of the normalized temporal velocity fluctuations $\boldsymbol{v}(t)$ are given by

$$\langle v_i(t) v_j(t') \rangle = \sigma_{vv}^2 C_{ij}^{vv}(t - t') \tag{20}$$

with the variance σ_{vv}^2 of the temporal fluctuations, which, for simplicity, is assumed to be equal in all directions. The correlations of the $v_i(t)$ are assumed to be short range, i.e., to decrease quickly for times larger than the correlation time τ.

Using decomposition (16) in (14), we obtain our working equation

$$\frac{\partial g(\mathbf{x},t)}{\partial t} + \mathbf{u}(t) \cdot \nabla g(\mathbf{x},t) - \nabla \mathbf{D} \nabla g(\mathbf{x},t) \rho(\mathbf{x}) \delta(t) + \mu(\mathbf{x}) \frac{\partial g(\mathbf{x},t)}{\partial t} + \mathbf{u}'(\mathbf{x},t) \cdot \nabla g(\mathbf{x},t). \tag{21}$$

2.4. Perturbation expansion

In the following we develop a perturbation expansion for $g(\mathbf{x},t)$ up to first-order in the variances of the random fields. (Note that ultimately one is expanding in the variances of the random fields, which in general need to be small for the perturbation results to be meaningful). This expansion serves as the basis for corresponding expansions for the effective transport velocity and dispersion coefficients.

2.4.1. Solute distribution

We reformulate the transport equation (21) in terms of an equivalent integral equation in Fourier space, from which we derive a perturbation solution of the transport problem. The Fourier transform $\tilde{g}(\mathbf{k},t)$ of $g(\mathbf{x},t)$ here is defined by

$$\tilde{g}(\mathbf{k},t) = \int \mathrm{d}^d x g(\mathbf{x},t) \exp(\mathrm{i}\mathbf{k} \cdot \mathbf{x}), \tag{22}$$

$$g(\mathbf{x},t) = \int_k \tilde{g}(\mathbf{k},t) \exp(-\mathrm{i}\mathbf{k} \cdot \mathbf{x}), \tag{23}$$

where Fourier-transformed quantities are marked by a tilde. Here and in the following we employ the short-hand notation,

$$\int_k \cdots = \int \frac{\mathrm{d}^d k}{(2\pi)^d} \cdots \tag{24}$$

The integral equation for $\tilde{g}(\mathbf{k},t)$ is given by (see e.g. [29,31])

$$\tilde{g}(\mathbf{k},t) = \tilde{g}_0(\mathbf{k},t,0)\tilde{\rho}(\mathbf{k}) + \int_{k'} \int_{-\infty}^{\infty} \mathrm{d}t' \tilde{g}_0(\mathbf{k},t,t') \mathbf{L}(\mathbf{k},\mathbf{k}',t') \tilde{g}(\mathbf{k}-\mathbf{k}',t'), \tag{25}$$

with the perturbation operator defined by,

$$\mathbf{L}(\mathbf{k},\mathbf{k}',t) \equiv \tilde{\mu}(\mathbf{k}') \frac{\partial}{\partial t} - \mathrm{i}\mathbf{k}\tilde{\mathbf{u}}'(\mathbf{k}',t'). \tag{26}$$

We used here the incompressibility condition $\mathbf{k} \cdot \tilde{\mathbf{u}}(\mathbf{k},t) = 0$. The Fourier-transformed Green function of the transport problem (21) for $\mu(\mathbf{x}) = 0$ and $\mathbf{u}'(\mathbf{x},t) = \mathbf{0}$, denoted in (25) by $\tilde{g}_0(\mathbf{k},t,t')$ reads as (e.g. [31]),

$$\tilde{g}_0(\mathbf{k},t,t') = \exp\left[-\mathbf{k}\mathbf{D}\mathbf{k}(t-t') + \mathrm{i}\mathbf{k} \cdot \int_{t'}^{t} \mathrm{d}\tau \mathbf{u}(\tau)\right] \Theta(t-t') \tag{27}$$

with $\Theta(t)$ the Heaviside step function as defined in [36].

Iteration of the integral equation (25) yields a perturbation series for $\tilde{g}(\mathbf{k},t)$ in terms of the perturbation operator $\mathbf{L}(\mathbf{k},\mathbf{k}',t)$,

$$\begin{aligned}\tilde{g}(\mathbf{k},t) = {} & \tilde{g}_0(\mathbf{k},t,0)\tilde{\rho}(\mathbf{k}) + \int_{k'} \int_{-\infty}^{\infty} \mathrm{d}t' \tilde{g}_0(\mathbf{k},t,t') \mathbf{L}(\mathbf{k},\mathbf{k}',t') \\ & \times \tilde{g}_0(\mathbf{k}-\mathbf{k}',t',0) + \int_{k'} \int_{-\infty}^{\infty} \mathrm{d}t' \int_{k''} \int_{-\infty}^{\infty} \mathrm{d}t'' \tilde{g}_0(\mathbf{k},t,t') \\ & \times \mathbf{L}(\mathbf{k},\mathbf{k}',t') \tilde{g}_0(\mathbf{k}-\mathbf{k}',t',t'') \times \mathbf{L}(\mathbf{k}-\mathbf{k}',\mathbf{k}'',t'') \\ & \times \tilde{g}_0(\mathbf{k}-\mathbf{k}''-\mathbf{k}'',t'',0) + \cdots.\end{aligned} \tag{28}$$

This series expansion truncated after the second-order in $\mathbf{L}$ constitutes the basis for the following perturbation analysis.

Note that the Green function $\tilde{g}_0(\mathbf{k},t,t')$, (27), depends on the temporal fluctuations $v_i(t)$. To obtain consistent expressions for the transport coefficients, $\tilde{g}_0(\mathbf{k},t,t')$ will be expanded in powers of $v(t)$ in the following (e.g. [29,31])

$$\tilde{g}_0(\mathbf{k},t,t') = \tilde{c}_0(\mathbf{k},t-t') \left[1 + u\mathrm{i}\mathbf{k} \cdot \int_{t'}^{t} \mathrm{d}t'' \boldsymbol{v}(t'') + \cdots\right] \Theta(t-t'). \tag{29}$$

We defined here

$$\tilde{c}_0(\mathbf{k},t) = \exp(-\mathbf{k}\mathbf{D}\mathbf{k}t + \mathrm{i}k_1 u t), \tag{30}$$

which is the Fourier transform of the solution of (21) for $\boldsymbol{v}(t) = \mathbf{u}'(\mathbf{x},t) \equiv \mathbf{0}$, and $\mu(\mathbf{x}) = 0$.

2.4.2. Transport coefficients

The effective transport velocity $u_i^{\mathrm{eff}}(t)$, (7), and the dispersion coefficients $D_{ij}^{\mathrm{eff}}(t)$, (8), can be expressed in terms of the Fourier transform of $p(\mathbf{x},t)$ as (e.g. [7,8])

$$u_i^{\mathrm{eff}}(t) = \frac{1}{\mathrm{i}} \frac{\mathrm{d}}{\mathrm{d}t} \frac{\partial}{\partial k_i} \langle \overline{\ln \tilde{p}(\mathbf{k},t)} \rangle|_{\mathbf{k}=\mathbf{0}} \tag{31}$$

$$D_{ij}^{\mathrm{eff}}(t) = -\frac{1}{2} \frac{\mathrm{d}}{\mathrm{d}t} \frac{\partial}{\partial k_i} \frac{\partial}{\partial k_j} \langle \overline{\ln \tilde{p}(\mathbf{k},t)} \rangle|_{\mathbf{k}=\mathbf{0}} \tag{32}$$

with the Fourier transform of $p(\mathbf{x},t)$ given by

$$\tilde{p}(\mathbf{k},t)=\frac{\tilde{g}(\mathbf{k},t)}{\tilde{g}(0,t)}. \tag{33}$$

Relations (31) and (32) can be readily verified by using the definition of the Fourier transform (23).

Inserting (28) into (32) and expanding the resulting expression for small variances of the random fields the dispersion coefficients decompose into,

$$D_{ij}^{\mathrm{eff}}(t)=D_{ij}+\delta^{\mu\mu}D_{ij}^{\mathrm{eff}}(t)+\delta^{uu}D_{ij}^{\mathrm{eff}}(t)+\delta^{u\mu}D_{ij}^{\mathrm{eff}}(t)+\delta^{u\nu}D_{ij}^{\mathrm{eff}}(t) \tag{34}$$

and accordingly for the effective center of mass velocity (31). Note that, strictly speaking, for such an expansion to be valid, the variances of the random fields are required to be small. The validity of such a simultaneous expansion in the variances of the spatial and temporal random fields has been discussed in [31].

The effective dispersion coefficient $D_{ij}^{\mathrm{eff}}(t)$ is given by the sum of the contributions due to (i) local dispersion D_{ij}, (ii) chemical heterogeneity $\delta^{\mu\mu}D_{ij}^{\mathrm{eff}}$ (see [7]), (iii) physical heterogeneity and temporal fluctuations of the flow conditions $\delta^{uu}D_{ij}^{\mathrm{eff}}$ (see e.g. [8,9,29,31]), (iv) cross-correlations between physical and chemical heterogeneity $\delta^{u\mu}D_{ij}^{\mathrm{eff}}$ (see e.g. [8] for the steady state case), and (v) the interaction between temporal fluctuations and chemical heterogeneity $\delta^{u\nu}D_{ij}^{\mathrm{eff}}$.

In the following, we focus on a physically homogeneous, chemically heterogeneous medium, which implies $\delta^{uu}D_{ij}^{\mathrm{eff}}=\delta^{u\mu}D_{ij}^{\mathrm{eff}}=0$. This kind of simplified model may be appropriate to describe the transport of an organic solute in an aquifer which is relatively homogeneous with respect to the hydraulic conductivity, but has a strongly varying organic carbon content (e.g. [28]).

Thus, we study $\delta^{u\nu}D_{ij}^{\mathrm{eff}}$ and its relative importance with respect to the contribution $\delta^{\mu\mu}D_{ij}^{\mathrm{eff}}$ due to chemical heterogeneity only [7]. Explicit expressions for $\delta^{u\nu}u_i^{\mathrm{eff}}$ and $\delta^{u\nu}D_{ij}^{\mathrm{eff}}$ are given in Appendix A.

2.4.3. Time scales and effective parameters

The temporal evolution of the effective dispersion coefficients is determined by three characteristic time scales, τ_u, τ_{D_i}, and τ_κ. The advection time scale τ_u measures the time for the solute to be advected over one longitudinal correlation length l_1,

$$\tau_u=\frac{l_1}{u}. \tag{35}$$

The dispersion time scales τ_{D_i} characterize the time for dispersive transport over one correlation length l_i,

$$\tau_{D_i}=\frac{l_i^2}{D_{ii}}. \tag{36}$$

The Kubo time scale τ_κ [31], measures the time for the local dispersive spreading over an effective length that is given by the correlation length l and the Kubo length $l_\kappa=u\tau$,

$$\tau_\kappa=(1+\kappa^2)\tau_{D_1}=(l^2+l_\kappa^2)\tau_{D_1}. \tag{37}$$

We defined here the non-dimensional Kubo number, $\kappa=\tau/\tau_u=l_\kappa/l_1$, which compares the correlation time τ to the advection time scale τ_u, and equivalently the Kubo distance $l_\kappa=u\tau$ (which denotes the length over which the solute is advected by the mean flow during one correlation time τ) to the correlation length in direction of the mean flow l_1.

The non-dimensional Peclet numbers $Pe_i=\tau_{D_i}/\tau_u$ compare the strength of advective and dispersive transport mechanism. In many hydrological applications transport is advection dominated, which implies large Peclet numbers, $Pe\gg 1$, or accordingly, small inverse Peclet numbers $\epsilon_i\equiv\tau_u/\tau_{D_i}=D_{ii}l_1/(ul_i^2)$. In the following we will develop simple compact expressions for the effective dispersion coefficients under the assumption of small ϵ_i.

Note that for times smaller than the advection timescale, $t\leqslant\tau_u$, the solute has moved by mean advection over a distance shorter than the correlation length l_1 of the medium, and has spread by local dispersion over a distance which is much smaller than the corresponding correlation distance. On such short scales the medium looks quasi homogeneous and the solute does not "see" the heterogeneity of the medium. Thus, the spatial ensemble average and accordingly the effective parameters defined as ensemble averages, have only a limited formal meaning for $t\leqslant\tau_u$ as there can be large sample to sample fluctuations between the disorder realizations. Correspondingly, for times smaller than the correlation time τ (or equivalently, for transport distances smaller than the Kubo distance l_κ), the flow field appears to be quasi steady, and the temporal average has only a formal meaning. The impact of spatial heterogeneity and temporal fluctuations can be quantified in terms of effective parameter only if the solute has sampled a representative part of the spectrum of spatio-temporal variability.

Appendix A summarizes the somewhat lengthy calculations that lead to the expressions for the effective center of mass velocity and dispersion coefficients presented in the following. We employ an expansion for small inverse Peclet numbers $\epsilon_i\ll 1$ and time large compared to the advection time scale $t\gg\tau_u$ (e.g. [31]) in order to simplify the lengthy expressions given in Appendix A.

2.4.3.1. Effective center of mass velocity. The leading contributions for small ϵ_i to the effective center of mass velocity, $\delta^{u\nu}u_i^{\mathrm{eff}}$, are given by (see Appendix A),

$$\delta^{u\nu}u_i^{\mathrm{eff}}(t)=u\sigma_{\mu\mu}^2\sigma_{\nu\nu}^2\int_{k'}\tilde{C}^{\mu\mu}(\mathbf{k}')[\delta_{i1}A(\mathbf{k}',t)+A_i(\mathbf{k}',t,0)]\times\exp(-\mathrm{i}uk_1't)+\cdots, \tag{38}$$

where the dots denote subleading contributions of the order of the inverse Peclet numbers. The auxiliary functions $A(\mathbf{k},t)$ and $A_i(\mathbf{k}',t,0)$ are defined by (A.18) and (A.19) in Appendix A. For short-range correlation functions, expression (38) decreases exponentially fast on the advection time scale τ_u.

2.4.3.2. Effective dispersion coefficients. As outlined in Appendix A, the leading behavior of $\delta^{\mu\nu}D_{ij}^{\text{eff}}(t)$ for small inverse Peclet numbers is given by,

$$\delta^{\mu\nu}D_{ij}^{\text{eff}}(t) = u^2\sigma_{\mu\mu}^2\sigma_{\nu\nu}^2\int_{k'}\int_0^t \mathrm{d}t'\tilde{C}^{\mu\mu}(\mathbf{k}')[\delta_{i1}\delta_{j1}A(\mathbf{k}',t') + \delta_{j1}A_i(\mathbf{k}',t',0) + \delta_{i1}A_j(\mathbf{k}',t',0) + C_{ij}^{\nu\nu}(t')] \times \exp(-\mathrm{i}uk_1't')[1-\exp(-2k_j'^2 l_j^2 t/\tau_{D_j})]. \quad (39)$$

3. Explicit expressions for the effective dispersion coefficients

We focus on a transport situation for which the temporal fluctuations are transverse to the direction of the mean flow velocity, $\boldsymbol{v}(t) = [0, v_2(t), \ldots, v_{\text{d}}(t)]^{\text{T}}$. In this case, (39) simplifies to,

$$\delta^{\mu\nu}D_{ij}^{\text{eff}}(t) = u^2\sigma_{\mu\mu}^2\sigma_{\nu\nu}^2\int_{k'}\int_0^t \mathrm{d}t'\tilde{C}^{\mu\mu}(\mathbf{k}') \times [\delta_{i1}\delta_{j1}A(k_2',\ldots,k_{\text{d}}',t') + C_{ij}^{\nu\nu}(t')p_ip_j] \times \exp(-\mathrm{i}uk_1't')[1-\exp(-2k_j'^2 l_j^2 t/\tau_{D_j})], \quad (40)$$

where we defined $p_i = (1-\delta_{i1})$. In the following, we study without loss of generality fluctuations in 2-direction, i.e.,

$$v_i(t) = \delta_{i2}v(t). \quad (41)$$

Using (41) in (20), the correlation matrix $C_{lm}^{\nu\nu}(t)$ reduces to,

$$C_{lm}^{\nu\nu}(t) = \delta_{l2}\delta_{m2}C^{\nu\nu}(t). \quad (42)$$

To derive explicit results, we need to specify the spatial and temporal correlation functions. The specific form of the spatial and temporal correlation functions $C^{\mu\mu}$ and $C^{\nu\nu}$ is to some extent arbitrary. A convenient choice made in the literature are Gauss-shaped functions. The temporal fluctuations of the flow field are assumed to be Gaussian correlated (e.g. [31]), i.e.,

$$C^{\nu\nu}(t) = \exp\left[-\frac{t^2}{2\tau^2}\right], \quad (43)$$

with τ the correlation time. In analogy to [7], we use a Gaussian shaped correlation function for the retardation field μ, which in Fourier space reads as,

$$C^{\mu\mu}(\mathbf{k}) = (2\pi)^{\frac{d}{2}}\prod_{i=1}^{d} l_i \exp\left[-\frac{1}{2}(k_il_i)^2\right]. \quad (44)$$

The length scales l_i are the correlation lengths of the retardation fields in direction i (with $i = 1,\ldots,d$).

Inserting (42) with (43) and (44) into (40) and using (A.18) for $A(k_2',t')$, we obtain,

$$\delta^{\mu\nu}D_{ii}^{\text{eff}}(t) = ul_1\sigma_{\mu\mu}^2\sigma_{\nu\nu}^2\int_{k'}\int_0^{t/\tau_u}\mathrm{d}t'\left[\delta_{i1}\frac{l_1^2}{l_2^2}\frac{k_2'^2}{2}\int_0^{t'}\mathrm{d}y\int_0^{t'}\mathrm{d}y' \times \exp\left[-\frac{(y-y')^2}{2\kappa^2}\right] + \delta_{i2}\exp\left(-\frac{t'^2}{2\kappa^2}\right)\right] \times \exp(-\mathrm{i}k_1't')\left\{1-\exp\left[-\frac{k_j'^2}{2}(1+4t/\tau_{D_j})\right]\right\}. \quad (45)$$

In the following we will restrict ourselves to isotropic disorder scenario, i.e., $l_1 = \cdots = l_{\text{d}}$. Then, for times large compared to the advection time scale τ_u, we obtain the following compact expressions for the effective dispersion coefficients,

$$\delta^{\mu\nu}D_{11}^{\text{eff}}(t) = \sqrt{\frac{\pi}{2}}\sigma_{\mu\mu}^2\sigma_{\nu\nu}^2 ul\frac{\kappa^2}{a(\kappa)}\left[a(\kappa) - 1 + \left[(1+4t/\tau_\kappa)^{\frac{1}{2}} - a(\kappa)\right] \times (1+4t/\tau_{D_2})^{-\frac{3}{2}}\prod_{n=3}^{d}(1+4t/\tau_{D_n})^{-\frac{1}{2}}\right], \quad (46)$$

$$\delta^{\mu\nu}D_{22}^{\text{eff}}(t) = \sqrt{\frac{\pi}{2}}\sigma_{\mu\mu}^2\sigma_{\nu\nu}^2 ula(\kappa)\left[1-(1+4t/\tau_\kappa)^{-\frac{1}{2}}\prod_{n=2}^{d}(1+4t/\tau_{D_n})^{-\frac{1}{2}}\right], \quad (47)$$

where we defined $a(\kappa) = \kappa/\sqrt{\kappa^2+1}$. The $\delta^{\mu\nu}D_{ii}^{\text{eff}} \equiv 0$ for $i > 2$ for symmetry reasons.

Note that $\delta^{\mu\nu}D_{11}^{\text{eff}} \leqslant 0$, while $\delta^{\mu\mu}D_{11}^{\text{eff}} + \delta^{\mu\nu}D_{11}^{\text{eff}} \geqslant 0$, for small $\sigma_{\nu\nu}^2$. For increasing $\sigma_{\nu\nu}^2$, this contribution can become negative, which, however, is a relic of the perturbation expansion in $\sigma_{\nu\nu}^2$, see Appendix A. Note that expansions in the fluctuations of the random fields can lead to non-convergent series for some transient non-linear reactive transport problems [38]. For the linear reactive transport problem under consideration here, however, the non-physical behavior of $\delta^{\mu\mu}D_{11}^{\text{eff}} + \delta^{\mu\nu}D_{11}^{\text{eff}} \leqslant 0$ is purely a relic of the small $\sigma_{\nu\nu}^2$ expansion.

For comparison we give here the explicit approximate expressions obtained by Attinger et al. [7] for $\delta^{\mu\mu}D_{ii}^{\text{eff}}$, in d dimensions,

$$\delta^{\mu\mu}D_{11}^{\text{eff}}(t) = \sqrt{\frac{\pi}{2}}\sigma_{\mu\mu}^2 ul\left[1-\prod_{n=2}^{d}\left(1+\frac{4t}{\tau_{D_n}}\right)^{-\frac{1}{2}}\right], \quad (48)$$

$$\delta^{\mu\mu}D_{ii}^{\text{eff}}(t) = 0. \quad (49)$$

Note, firstly, that the time evolution of $\delta^{\mu\mu}D_{11}^{\text{eff}}$ depends only on the transverse dispersion scale, and secondly that there is no macroscopic contribution to the transverse dispersion coefficient.

4. Effective transport behavior

It was shown by Attinger et al. [7] for transport under steady flow conditions that chemical medium heterogeneities change the behavior of the longitudinal dispersion coefficient in a quantitatively relevant way, whereas transverse solute spreading is only weakly influenced by the fluctuations of the retardation factor. As we saw at the end of the previous section, the effective transverse dispersion coefficient is in fact of the order of the local dispersion coefficient. For transport under a temporally fluctuating flow conditions, the behavior of transverse and longitudinal effective dispersion coefficients is different.

In the following, we investigate the asymptotic long time behavior and the temporal evolution of the effective disper-

sion coefficients in $d = 2$ dimensions. All results are normalized by $\sqrt{\frac{\pi}{2}}\sigma^2_{\mu\mu}\sigma^2_{vv}ul$. The behavior in $d = 3$ dimensions is qualitatively similar.

4.1. Asymptotic long time behavior

We study here the asymptotic behavior of the contributions to the effective dispersion coefficients for isotropic local dispersion, $D_{11} = D_{22} = D$, as a function of the Kubo number κ. We define for the following,

$$\lim_{t\to\infty} \delta^{\mu v} D^{\text{eff}}_{11}(t) = \delta^{\mu v} D^{\infty}_{11}(\kappa), \tag{50}$$

$$\lim_{t\to\infty} \delta^{\mu v} D^{\text{eff}}_{22}(t) = \delta^{\mu v} D^{\infty}_{22}(\kappa). \tag{51}$$

Fig. 1 illustrates the asymptotic behavior of $\delta^{\mu v} D^{\infty}_{22}(\kappa)$ and $\delta^{\mu v} D^{\infty}_{11}(\kappa)$. Both contributions to the longitudinal and transverse effective dispersion coefficients tend to zero in the limit $\kappa \to 0$. In this limit, the correlation time τ is much smaller than the advection time τ_u, or equivalently, the Kubo length is much smaller than the correlation length, $l_\kappa \ll l$. Thus, for many correlation times, the medium looks quasi homogeneous to the transported solute and, as shown by Dentz and Carrera [29], there are no contributions to effective solute spreading due to temporal velocity fluctuations in homogeneous media.

For $\kappa \ll 1$, $\delta^{\mu v} D^{\infty}_{22}(\kappa)$ increases linearly,

$$\delta^{\mu v} D^{\infty}_{22}(\kappa) = \sqrt{\frac{\pi}{2}}\sigma^2_{\mu\mu}\sigma^2_{vv}ul\kappa, \tag{52}$$

as illustrated in Fig. 1. In this regime, the Kubo length is of the order of the spatial correlation length, $l_\kappa \lesssim l$, i.e., the solute samples the spatial heterogeneity during one "fluctuation cycle" (i.e., within the correlation time), which leads to enhanced spreading in transverse direction.

$\delta^{\mu v} D^{\infty}_{11}(\kappa)$, in contrast, decreases linearly in the same κ-interval,

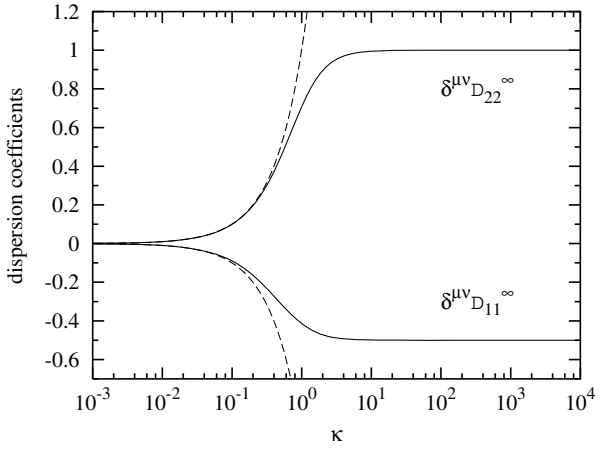

Fig. 1. Asymptotic behavior of the contributions to the effective dispersion coefficients due to chemical heterogeneity and temporal fluctuations in solid lines. The dashed lines describe the behavior of $\delta^{\mu v} D^{\infty}_{22}$ and $\delta^{\mu v} D^{\infty}_{11}$ according to (52) and (53), respectively.

$$\delta^{\mu v} D^{\infty}_{11}(\kappa) = -\frac{1}{2}\sqrt{\frac{\pi}{2}}\sigma^2_{\mu\mu}\sigma^2_{vv}ul\kappa, \tag{53}$$

see Fig. 1. The contribution to the longitudinal effective dispersion coefficient decreases as the transverse coefficient is increasing. This will be discussed in the following.

In contrast to transport under steady flow conditions, where the disorder-induced contribution to effective transverse dispersion is of the order of local dispersion, here $\delta^{\mu v} D^{\infty}_{22}$ is macroscopic and dependent on the Kubo number κ. At the same time, the longitudinal dispersion coefficient decreases as $\delta^{\mu v} D^{\infty}_{11}$ is negative as shown in Fig. 1. The simultaneous increase of the transverse and decrease of the longitudinal effective dispersion coefficients can be seen as a consequence of self-organization of the system. Increased transverse spreading smoothes the concentration contrasts along directions normal to the mean flow, which in turn leads to a decrease of longitudinal effective spreading. A similar mechanism is known for the Taylor problem of dispersion in shear flow [37]. There, solute dispersion is enhanced as a consequence of the fact that the solute samples the transverse velocity contrast in the direction vertical to the mean flow. Vertical concentration contrasts, which lead to enhanced spreading, are smaller for increasing transverse dispersion. Thus, an increase of the transverse dispersion leads to a decrease of the Taylor dispersion coefficient.

4.2. Time behavior

We study the time evolution of the contributions to the effective dispersion coefficient using the explicit expressions (46) and (47) for the longitudinal and transverse dispersion coefficients, respectively. We investigate different scenarios in order to study the different mechanisms which affect the behavior of the effective dispersion coefficients. At first we investigate an isotropic scenario for small and large Kubo numbers. Secondly, we investigate an anisotropic local dispersion scenario varying the longitudinal local dispersion coefficient.

4.2.1. Isotropic scenario

For the isotropic scenario, the inverse Peclet numbers ϵ_i and the dispersion time scales τ_{D_i} reduce to $\epsilon_i = \epsilon$ and $\tau_{D_i} = \tau_D$ for $i = 1, \ldots, d$.

Figs. 2a and 2b illustrate the time evolution of the contributions $\delta^{\mu v} D^{\text{eff}}_{22}$ to the transverse and $\delta^{\mu v} D^{\text{eff}}_{11}$ to the longitudinal effective dispersion coefficients in $d = 2$ for $\kappa = 10^{-1}$ and $\kappa = 10$. The dispersion time scale is $\tau_D = 10^3\tau_u$, i.e., the advection and dispersion time scales τ_u and τ_D are clearly separated.

For large values of κ, corresponding to $\tau_\kappa \gg \tau_D$, the Kubo scale τ_κ together with τ_u and τ_D, separates three different time regimes: (i) the intermediate time regime $\tau_u \ll t \ll \tau_D$, (ii) the Kubo time regime $\tau_D \ll t \ll \tau_\kappa$, and (iii) the long-time regime $t \gg \tau_\kappa$. The Kubo scale sets a rel-

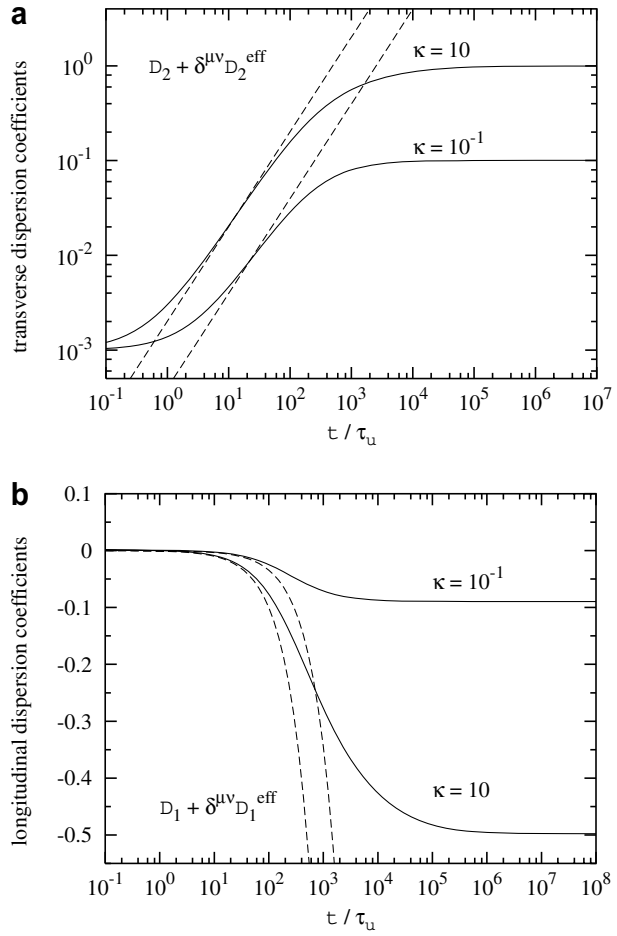

Fig. 2. Time behavior of the contributions to the (a) transverse effective dispersion coefficients, (b) longitudinal effective dispersion coefficients, in $d = 2$ for $\tau_D = 10_3\ \tau_u$, $\epsilon = 10^{-3}$, $t \gg \tau_u$, $\kappa = 10^{-1}$ and $\kappa = 10$. The dashed lines in (a) and (b) describe the linear approximations (54) and (55) of $\delta^{\mu\nu} D_{22}^{\text{eff}}$ and $\delta^{\mu\nu} D_{11}^{\text{eff}}$, respectively.

evant asymptotic time scale. Note that the solute has to be spread by local dispersion over at least one correlation length of the medium to "see" the chemical heterogeneity and it has to be spread over at least one Kubo length l_κ to notice the influence of temporal flow fluctuations. Note that for small κ, $\tau_\kappa \approx \tau_D$, see definition (37), i.e., the Kubo scale is of importance for large Kubo numbers only. In order to illustrate this feature, we choose $\kappa = 10^{-1}$ and $\kappa = 10$.

(i) *Intermediate time regime* $\tau_u \ll t \ll \tau_D$

In this time regime, spatial heterogeneity is being activated as a macroscopic spreading mechanism and we observe a cross-over from local dispersive spreading and mixing to macroscopic heterogeneity induced effective dispersion. The contribution to the effective transverse dispersion coefficient, $\delta^{\mu\nu} D_{22}^{\text{eff}}$, both for $\kappa = 10^{-1}$ and $\kappa = 10$ evolves linearly with time,

$$\delta^{\mu\nu} D_{22}^{\text{eff}}(t) = \sqrt{2\pi}\sigma_{\mu\mu}^2 \sigma_{\mu\nu}^2 ula(\kappa) \frac{(\kappa^2+2)}{(\kappa^2+1)} \frac{t}{\tau_D} + \cdots, \tag{54}$$

where the dots denote subleading contributions. Contrary to the behavior observed under steady flow conditions, where transverse spreading is mainly given by local dispersion, here the transverse dispersion coefficient grows from the (microscopic) local scale dispersion coefficient to a macroscopic value. As shown in Fig. 2b, the contribution to the longitudinal coefficient decreases linearly according to,

$$\delta^{\mu\nu} D_{11}^{\text{eff}}(t) = -\sqrt{2\pi}\sigma_{\mu\mu}^2 \sigma_{\mu\nu}^2 ula(\kappa) \left[2 + 3\kappa(\kappa - \sqrt{\kappa^2+1})\right] \frac{t}{\tau_D} + \cdots, \tag{55}$$

towards a negative macroscopic value and thus, longitudinal effective dispersion decreases as discussed in Section 4.1.

(ii) *Kubo time regime* $\tau_D \ll t \ll \tau_\kappa$

For $\kappa = 10$, $\delta^{\mu\nu} D_{22}^{\text{eff}}$, see Fig. 2a, evolves approximately according to $t^{-1/2}$, which is identical to the behavior observed for the longitudinal component under steady state conditions [7]. For $\kappa = 10^{-1}$, i.e., $\tau_\kappa \approx \tau_D$ and the Kubo and long time regimes coincide. The contribution $\delta^{\mu\nu} D_{22}^{\text{eff}}$ evolves as t^{-1} towards its asymptotic macroscopic value. The difference in the behaviors for $\kappa = 10^{-1}$ and 10 can be well observed in Fig. 2a. For $\kappa = 10^{-1}$ the evolution of the $\delta^{\mu\nu} D_{22}^{\text{eff}}$ is faster than for $\kappa = 10$. Note that for times, $\tau_D \ll t \ll \tau_\kappa$, the solute has spread out over a distance larger than the correlation length l, hence, the solute has sampled a representative part of the chemical heterogeneity. However, for large Kubo numbers, the Kubo length is much larger than the correlation length, $l_\kappa \gg l$, i.e., the solute has been transported over more than one correlation length without noticing the temporal variability of the flow. Thus spreading is dominated by the interaction of local dispersion and chemical heterogeneities, and the behavior of $\delta^{\mu\nu} D_{22}^{\text{eff}}$ is similar to the one observed for the longitudinal dispersion coefficient under steady flow conditions as in this time regime, $v(t)$ is approximately constant, i.e., there is an approximately constant transverse velocity component. For $\kappa = 10^{-1}$, the solute has spread by local dispersion over distances larger than both, the correlation length and the Kubo length. Thus, both spatial heterogeneity as well as temporal flow fluctuations are activated as macroscopic spreading mechanisms. For this reason $\delta^{\mu\nu} D_{22}^{\text{eff}}$ evolves faster for $\kappa = 10^{-1}$ than for $\kappa = 10$. The same behavior can be observed in Fig. 2 for $\delta^{\mu\nu} D_{11}^{\text{eff}}$, which decreases faster for $\kappa = 10^{-1}$ than for $\kappa = 10$ for the reasons given above.

(iii) *Long time regime* $t \gg \tau_\kappa$

As pointed out above, for $\kappa = 10^{-1}$, the Kubo and long time regimes coincide. For $\kappa = 10$, the long time regime is set by the Kubo scale, see Figs. 2a and 2b. As pointed out above, only when the solute has been spread out over distances which are larger than both the correlation and the Kubo lengths, the interaction between chemical heterogeneity and temporal fluctuations are activated as macroscopic spreading mechanisms. As discussed above for $\kappa = 10^{-1}$, here both $\delta^{\mu\nu} D_{22}^{\text{eff}}$ and $\delta^{\mu\nu} D_{11}^{\text{eff}}$ evolve towards their respective asymptotic values according to t^{-1}, i.e., faster

than the contribution $\delta^{\mu\mu}D_{11}^{\text{eff}}$ in the absence of temporal flow fluctuations.

4.2.2. Anisotropic scenario

Here we study the temporal behavior of the effective dispersion coefficients for anisotropic local dispersion and isotropic disorder correlation.

Fig. 3a and b illustrate the time behavior of $\delta^{\mu v}D_{22}^{\text{eff}}$ and $\delta^{\mu v}D_{11}^{\text{eff}}$ for a fixed $\epsilon_1 = 10^{-1}$ and varying ϵ_2 of $\epsilon_2 = 10^{-7}$, 10^{-6}, 10^{-5} and $\epsilon_2 = 10^{-4}$, in $d = 2$, for $\kappa = 1$. The temporal behavior of $\delta^{\mu v}D_2^{\text{eff}}(t)$ is plotted only for the cases $\epsilon_2 = 10^{-7}$ and $\epsilon_2 = 10^{-4}$. For the values in between, the curves are basically identical.

For the isotropic scenario discussed in Section 4.2.1, $\tau_\kappa \geqslant \tau_D$ and the asymptotic long time regime was defined by the Kubo time scale τ_κ. For the anisotropic scenario under consideration here, the Kubo scale is smaller than the transverse dispersion time scale, $\tau_\kappa \ll \tau_{D_2}$. Thus, τ_{D_2} defines the relevant asymptotic time scale. These two time scales, along with the advection scale, define three time regimes which characterize the interaction of local dispersion, spatial heterogeneity and temporal fluctuations: (i) the Kubo time regime $\tau_u \ll t \ll \tau_\kappa$, (ii) the intermediate time regime $\tau_\kappa \ll t \ll \tau_{D_2}$, and (iii) the long-time regime $t \gg \tau_{D_2}$.

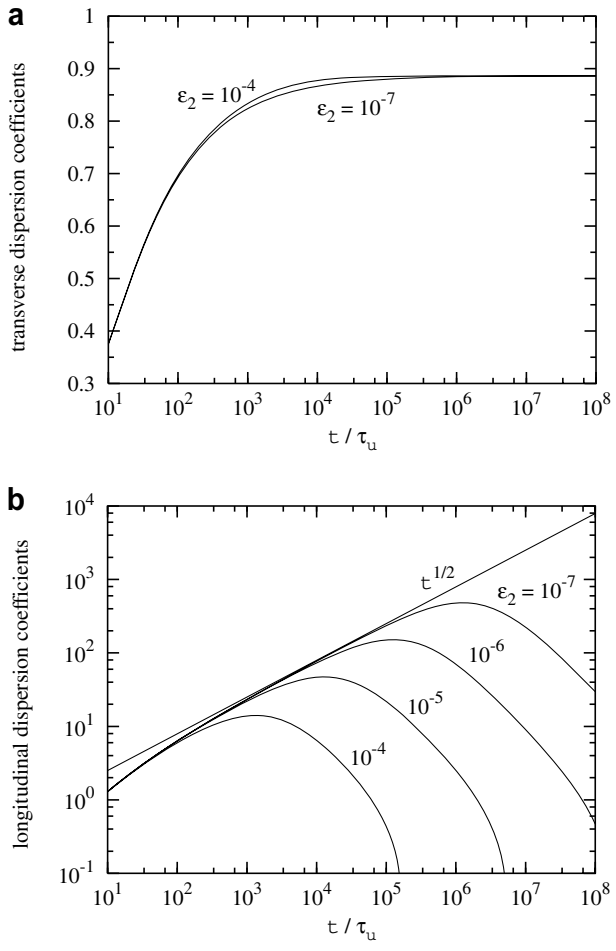

Fig. 3. Time behavior of (a) $\delta^{\mu v}D_{22}^{\text{eff}}(t)$, and (b) $\delta^{\mu v}D_{11}^{\text{eff}}$ (both scaled by $\sqrt{\frac{\pi}{2}}\sigma_{\mu\mu}^2\sigma_{vv}^2 ul$) in $d = 2$ for $\kappa = 1$ and a fixed $\epsilon_1 = 10^{-1}$; ϵ_2 varies between 10^{-7} and 10^{-4}.

(i) *Kubo time regime* $\tau_u \ll t \ll \tau_\kappa$.

In this time regime, the solute has been transported by advection over a distance larger than the correlation length l of the chemically heterogeneous medium. Solute has not been spread by local dispersion over distances larger than both the correlation length l and the Kubo length l_κ. In this regime, temporal fluctuations and spatial heterogeneity are activated as relevant macroscopic spreading mechanism and we observe a cross-over from microscopic local dispersion to macroscopic disorder-induced spreading and mixing. The $\delta^{\mu v}D_{22}^{\text{eff}}$ and $\delta^{\mu v}D_{11}^{\text{eff}}$, see Figs. 3a and 3b, evolve linearly with time, as observed in the isotropic scenario.

(ii) *Intermediate time regime* $\tau_\kappa \ll t \ll \tau_{D_2}$.

Here, the solute has spread by longitudinal local dispersion over the Kubo length l_κ. In transverse direction, however, the solute has not yet sampled one spatial correlation length of the medium by transverse local dispersion.

The evolution of $\delta^{\mu v}D_{22}^{\text{eff}}$ for $\epsilon = 10^{-4}$ is different from the one observed for $\epsilon_2 = 10^{-7}$. For $\epsilon_2 = 10^{-4}$, $\delta^{\mu v}D^{\text{eff}}D_{22}$ evolves faster towards its asymptotic long time value as transverse local dispersive mixing is more efficient.

The evolution of $\delta^{\mu v}D_{11}^{\text{eff}}$ depends strongly on the value ϵ_2. In this time regime, $\delta^{\mu v}D_{11}^{\text{eff}}$ evolves as $t^{1/2}$ towards a maximum, which it assumes for times of about $10^{-1}\tau_{D_2}$. For steady flow conditions, transport would be quasi unidimensional in this regime, as local transverse dispersion is subleading. In the presence of transverse flow fluctuations, however, there is vertical mass exchange. The transverse heterogeneity contrasts encountered by the solute leads then to the anomalous $t^{1/2}$ growth of $\delta^{\mu v}D_{11}^{\text{eff}}$. Note that local transverse dispersion, which smoothes out these vertical contrasts, is subleading. The anomalous diffusive behavior found here is similar to the one observed in stratified flow (e.g. [39,40]). The mechanisms are similar, but slightly different. While in the case of the stratified medium, local transverse dispersion is the vertical solute spreading and mixing mechanisms that leads, in interaction with the vertical velocity contrast, to the characteristic $t^{1/2}$ growth of the longitudinal effective dispersion coefficient, here transverse flow fluctuations cause vertical mass exchange. These mechanisms, local dispersion and transverse flow fluctuations, are different.

(iii) *Long time regime* $t \gg \tau_{D_2}$.

Here, the solute has spread over a correlation length of the medium by transverse local dispersion. Thus, spatial heterogeneity has been activated as a macroscopic spreading mechanism. The $\delta^{\mu v}D_{22}^{\text{eff}}$ converges towards its macroscopic asymptotic long time value. As a consequence of the increase in transverse effective dispersion, which leads to a smoothing out of the vertical heterogeneity contrast,

$\delta^{\mu\nu} D_{11}^{\text{eff}}$, decreases towards its asymptotic long time value. The transverse dispersion time scale τ_{D_2} is a cut-off time scale for the anomalous diffusive behavior observed in the previous time regime.

5. Summary and conclusions

We investigate the effective transport of a reactive solute evolving from a point-like injection through a chemically heterogeneous medium. We focus on spatially fluctuating equilibrium sorption properties, which are characterized by a random retardation factor. The flow velocity is fluctuating in time with fluctuations transverse to the mean flow direction. In a stochastic modeling framework the spatial heterogeneity and temporal flow fluctuations are modeled by means of correlated spatial and temporal random fields.

The effective transport behavior is studied in terms of effective dispersion coefficients, which quantify the impact of spatio-temporal fluctuations on effective solute spreading and mixing. Using a first-order perturbation approach in the variances of the random processes, we derive explicit compact expressions for the time behavior of the transverse and longitudinal effective dispersion coefficients.

The effective dispersion coefficients are given as the sum of the contributions due to (i) local dispersion, (ii) the interaction of local dispersion and chemical heterogeneity, (iii) the interaction of local dispersion physical heterogeneity and temporal flow fluctuations, (iv) the interaction of local dispersion and cross-correlations between physical and chemical heterogeneity, and (v) the interaction between local dispersion, temporal fluctuations and chemical heterogeneity. Here we focus on a physically homogeneous, chemically heterogeneous medium and study the latter contribution.

The time behavior of the effective dispersion coefficients are dominated by the following time scales: (i) the advection time scale $\tau_u = l/u$, (ii) the dispersion time scale $\tau_{D_2} = l/D_{22}$, which gives the activation time scale for chemical heterogeneities as a relevant macroscopic spreading mechanism, and (iii) the Kubo time scale $\tau_\kappa = (l^2 + l_\kappa^2)/D_{11}$ which measures the time for the local dispersive spreading over a distance larger than both the correlation length l and the Kubo length, $l_\kappa = u\tau$. Only after the time τ_κ, the interaction between chemical heterogeneities and temporal flow fluctuations is activated as a macroscopic spreading mechanism.

Due to the interaction of temporal flow fluctuations and chemical heterogeneity, transverse effective dispersion evolves towards a macroscopic asymptotic value, which is in sharp contrast to the corresponding results for steady flow conditions, where no macroscopic contribution to transverse effective dispersion has been found.

In order to study the different spreading and mixing mechanisms and the interaction between them, we analyze two scenarios in $d = 2$ spatial dimensions, (i) a completely isotropic scenario characterized by isotropic local dispersion and disorder correlation, and (ii) a scenario characterized by an isotropic correlation structure and anisotropic local dispersion.

In the isotropic scenario, we distinguish three regimes, (i) the intermediate time regime $\tau_u \ll t \ll \tau_D$, (ii) the Kubo time regime $\tau_D \ll t \ll \tau_\kappa$ and (iii) the long time regime $t \gg \tau_\kappa$. In the intermediate regime, the plume size is still smaller than a disorder correlation length. Thus spatial heterogeneity has not been activated as an effective spreading mechanism. In the Kubo regime, the plume is larger than the disorder correlation length, but smaller than the Kubo-length. Thus, spatial heterogeneity is activated as a macroscopic spreading mechanism, time fluctuations are not. Only in the asymptotic regime, both spatial heterogeneity and temporal fluctuations are activated as effective spreading mechanisms.

For the anisotropic scenario we consider a different order of time scales, which implies (i) $\tau_\kappa \ll t \ll \tau_{D_2}$ and (ii) $t \gg \tau_{D_2}$. For $\tau_\kappa \ll t \ll \tau_{D_2}$, we observe superdiffusive behavior for the longitudinal effective dispersion coefficient. In this regime, transverse local dispersion is subleading and cannot smooth out the vertical concentration contrasts induced by the interaction of transverse redistribution of the solute by the temporal flow fluctuations and spatial heterogeneity. As soon as the plume has spread over more than one vertical correlation length by local transverse dispersion for $t > \tau_D$, longitudinal effective dispersion becomes normal.

The studied effective dispersion behavior and the analysis of the different micro and macroscopic spreading mechanisms and the interaction between them sheds some new light on the understanding of effective transport processes in heterogeneous media. The observed increase of transverse dispersion due to temporal flow fluctuations can have important practical implications for the assessment of groundwater remediation based on hydraulic manipulation, as well as for the assessment and prediction of the migration of reactive contaminants in the context of performance assessment in nuclear waste management. The developed compact and simple expressions for the effective dispersion coefficients can be easily used for the quantification of effective solute spreading and mixing in such applications.

Acknowledgments

V.Z. gratefully acknowledges the financial support of the European Commission and the Departament d'Universitats, Recerca i Societat de la Informació de la Generalitat de Catalunya. M.D. gratefully acknowledges the support of the program 'Ramon y Cajal' of the Spanish Ministry of Education and Science (MEC). The finicial support by ENRESA and the EU through the IP FUNMIG (Contract No. 516514) and the MEC through the project MODEST (Contract No. CGL-2005-05171) is gratefully acknowledged.

Appendix A. Integral expressions

Here we present the explicit integral expressions for the contributions to the effective transport velocity and the effective dispersion coefficients due to the interaction between temporal fluctuations of the flow conditions and chemical heterogeneity.

We derive approximate expressions for small inverse Peclet numbers. In order to keep the derivations as transparent as possible, the derived expressions are approximated successively, which means that, in the course of the derivations, we successively disregard subleading terms until we arrive at the consistent final result that represents the leading behavior in the limit of small inverse Peclet numbers.

Inserting expansion (28) for $\tilde{g}(\mathbf{k},t)$ into $\overline{\ln[\tilde{g}(\mathbf{k},t)]}$ and expanding the resulting expression up to first order in $\sigma^2_{\mu\mu}$, we obtain

$$\overline{\ln[\tilde{g}(\mathbf{k},t)]} = g_0(\mathbf{k},t) + \sigma^2_{\mu\mu}[I_1(\mathbf{k},t) + I_2(\mathbf{k},t)] \tag{A.1}$$

and thus for the effective center of mass velocity (31) and the effective dispersion coefficients (32),

$$u_i^{\mathrm{eff}}(t) = u\delta_{i1} - \sigma^2_{\mu\mu}\frac{\mathrm{d}}{\mathrm{d}t}\mathrm{i}\frac{\partial}{\partial k_i}\left[\langle I_1(\mathbf{k},t)\rangle - \frac{1}{2}\langle I_2(\mathbf{k},t)\rangle\right]_{\mathbf{k}=\mathbf{0}}, \tag{A.2}$$

$$D_{ij}^{\mathrm{eff}}(t) = D_{ij} - \sigma^2_{\mu\mu}\frac{1}{2}\frac{\mathrm{d}}{\mathrm{d}t}\frac{\partial^2}{\partial k_i \partial k_j}\left[\langle I_1(\mathbf{k},t)\rangle - \frac{1}{2}\langle I_2(\mathbf{k},t)\rangle\right]_{\mathbf{k}=\mathbf{0}}. \tag{A.3}$$

The auxiliary functions $I_1(\mathbf{k},t)$ and $I_2(\mathbf{k},t)$ are defined by

$$I_1(\mathbf{k},t) = \frac{1}{\tilde{g}_0(\mathbf{k},t,0)}\int_{k'}\int_{-\infty}^{\infty}\mathrm{d}t'\int_{-\infty}^{\infty}\mathrm{d}t''C^{\mu\mu}(\mathbf{k}')\tilde{g}_0(\mathbf{k},t,t') \times\frac{\partial}{\partial t'}\tilde{g}_0(\mathbf{k}-\mathbf{k}',t',t'')\frac{\partial}{\partial t''}\tilde{g}_0(\mathbf{k},t'',0), \tag{A.4}$$

$$I_2(\mathbf{k},t) = \frac{1}{\tilde{g}_0(\mathbf{k},t,0)^2}\int_{k'}\int_{-\infty}^{\infty}\mathrm{d}t'\int_{-\infty}^{\infty}\mathrm{d}t''C^{\mu\mu}(\mathbf{k}')\tilde{g}_0(\mathbf{k},t,t') \times\frac{\partial}{\partial t'}\tilde{g}_0(\mathbf{k}-\mathbf{k}',t',0)\tilde{g}_0(\mathbf{k},t,t'')\frac{\partial}{\partial t''}\tilde{g}_0(\mathbf{k}+\mathbf{k}',t'',0), \tag{A.5}$$

respectively. By partially integrating with respect to t' and t'', the internal time derivatives are shifted to the propagators that contain only external wave vectors $\mathbf{k}$. Evaluating the resulting time derivatives, we obtain for $I_1(\mathbf{k},t)$ and $I_2(\mathbf{k},t)$

$$\begin{aligned} I_1(\mathbf{k},t) &= I_{11}(\mathbf{k},t) + I_{12}(\mathbf{k},t) + I_{13}(\mathbf{k},t) + \cdots,\\ I_2(\mathbf{k},t) &= I_{21}(\mathbf{k},t) + 2I_{22}(\mathbf{k},t) + \cdots, \end{aligned} \tag{A.6}$$

where the dots denote contributions which are small for small inverse Peclet numbers and contributions that are independent of $\mathbf{k}$. The auxiliary functions contributing to $I_1(\mathbf{k},t)$ are defined by

$$I_{11}(\mathbf{k},t) = -\int_{k'}\int_0^t\mathrm{d}t'\int_0^{t'}\mathrm{d}t''\mathbf{k}\cdot\mathbf{u}(t')\mathbf{k}\cdot\mathbf{u}(t'')B_1(\mathbf{k}',t',t''), \tag{A.7}$$

$$I_{12}(\mathbf{k},t) = \int_{k'}\int_0^t\mathrm{d}t'\mathrm{i}\mathbf{k}\cdot\mathbf{u}(t')B_1(\mathbf{k}',t',0), \tag{A.8}$$

$$I_{13}(\mathbf{k},t) = \int_{k'}\int_0^t\mathrm{d}t'\mathrm{i}\mathbf{k}\cdot\mathbf{u}(t')B_1(\mathbf{k}',t,t'), \tag{A.9}$$

where we defined

$$B_1(\mathbf{k}',t_1,t_2) = \tilde{C}^{\mu\mu}(\mathbf{k}')\tilde{c}_0(-\mathbf{k}',t_1-t_2)[h(\mathbf{k}',t_1,t_2)+1] \tag{A.10}$$

with

$$h(\mathbf{k}',t_1,t_2) = \exp\left[-\mathrm{i}u\mathbf{k}'\int_{t_2}^{t_1}\mathrm{d}y\boldsymbol{v}(y)\right] - 1. \tag{A.11}$$

The auxiliary functions contributing to $I_2(\mathbf{k},t)$ are given by

$$I_{21}(\mathbf{k},t) = -\int_{k'}\int_0^t\mathrm{d}t'\int_0^t\mathrm{d}t''\mathbf{k}\cdot\mathbf{u}(t')\mathbf{k}\cdot\mathbf{u}(t'')B_2(\mathbf{k}',t',t''), \tag{A.12}$$

$$I_{22}(\mathbf{k},t) = \int_{k'}\int_0^t\mathrm{d}t'\mathrm{i}\mathbf{k}\cdot\mathbf{u}(t')B_2(\mathbf{k}',t,t'), \tag{A.13}$$

where we defined

$$B_2(\mathbf{k}',t_1,t_2) = \tilde{C}^{\mu\mu}(\mathbf{k}')\tilde{c}_0(-\mathbf{k}',t_1)\tilde{c}_0(\mathbf{k}',t_2)[h(\mathbf{k}',t_1,t_2)+1]. \tag{A.14}$$

Note that the contributions $I_{11}(\mathbf{k},t)$ and $I_{21}(\mathbf{k},t)$ are of second order in $\mathbf{k}$ and contribute only to the effective dispersion coefficients, while $I_{12}(\mathbf{k},t)$ and $I_{22}(\mathbf{k},t)$ are linear in $\mathbf{k}$ and thus contribute only to the effective center of mass velocity.

The determination of the effective center of mass velocity and dispersion coefficients involves the following averages:

$$\langle h(t_1,t_2)\rangle = \sigma^2_{vv}A(\mathbf{k}',t_1-t_2)+\cdots, \tag{A.15}$$

$$\langle v_l(t_3)h(t_1,t_2)\rangle = \sigma^2_{vv}A_l(\mathbf{k}',t_1-t_2,t_3-t_2)+\cdots, \tag{A.16}$$

$$\langle v_l(t_3)v_{\mathrm{m}}(t_4)h(t_1,t_2)\rangle = \sigma^2_{vv}C^{vv}_{lm}(t_3-t_4)+\cdots, \tag{A.17}$$

where the dots denote contributions of the order of σ^4_{vv}. We defined the auxiliary functions

$$A(\mathbf{k}',t) = -\frac{u^2}{2}\int_0^t\mathrm{d}y\int_0^t\mathrm{d}y'k'_lC^{vv}_{lm}(y-y')k'_{\mathrm{m}}, \tag{A.18}$$

$$A_l(\mathbf{k}',t_1,t_2) = -\mathrm{i}u\int_0^{t_1}\mathrm{d}yC^{vv}_{lm}(t_2-y)k'_{\mathrm{m}}. \tag{A.19}$$

The average over $h(t_1,t_2)$ can be performed exactly for a Gaussian distributed $\boldsymbol{v}(t)$. This yields,

$$\langle h(t_1,t_2)\rangle = \exp\left[-\sigma^2_{vv}\frac{u^2}{2}\int_{t_2}^{t_1}\mathrm{d}y\int_{t_2}^{t_1}\mathrm{d}y'k'_lC^{vv}_{lm}(y-y')k'_{\mathrm{m}}\right] - 1. \tag{A.20}$$

Note that (A.20) is always positive, while the first order approximation of this expression in σ^2_{vv} can be negative. Expression (A.20) gives the sum of $\delta^{\mu\mu}D^{\mathrm{eff}}_{11} + \delta^{\mu\nu}D^{\mathrm{eff}}_{11}$ and is always positive. The contribution (47) has been obtained by the first-order expansion of (A.20) and is

strictly valid only for small variances at which $\delta^{\mu\mu}D_{11}^{\text{eff}} + \delta^{\mu\nu}D_{11}^{\text{eff}} \geqslant 0$.

In fact, the first-order approximation of (A.20) leads to unphysical negative values for the effective longitudinal dispersion coefficients for increasing variance.

Inserting (A.8), (A.9) and (A.13) into (A.2), expansion up to second order in the temporal fluctuations and subsequent average over the temporal random fields, we obtain for the effective center of mass velocity,

$$u_i^{\text{eff}}(t) = u\delta_{i1} + \delta^{\mu\mu}u_i^{\text{eff}}(t) + \delta^{\mu\nu}u_i^{\text{eff}}(t) \tag{A.21}$$

with the contributions,

$$\delta^{\mu\mu}u_i^{\text{eff}}(t) = u\delta_{i1}\sigma_{\mu\mu}^2\int_{k'}\tilde{C}^{\mu\mu}(\mathbf{k}')\tilde{c}_0(-\mathbf{k}',t) + \cdots, \tag{A.22}$$

$$\delta^{\mu\nu}u_i^{\text{eff}}(t) = u\sigma_{\mu\mu}^2\sigma_{\nu\nu}^2\int_{k'}\tilde{C}^{\mu\mu}(\mathbf{k}')[\delta_{i1}A(\mathbf{k}',t) + A_i(\mathbf{k}',t,0)]\tilde{c}_0(-\mathbf{k}',t) + \cdots, \tag{A.23}$$

where again the dots denote contributions that are small for small inverse Peclet numbers.

Correspondingly, we obtain for the effective dispersion coefficients by inserting (A.7) and (A.12) into (A.3),

$$D_{ij}^{\text{eff}}(t) = D_{ij} + \delta^{\mu\mu}D_{ij}^{\text{eff}}(t) + \delta^{\mu\nu}D_{ij}^{\text{eff}}(t), \tag{A.24}$$

where we defined,

$$\delta^{\mu\mu}D_{ij}^{\text{eff}}(t) = u^2\sigma_{\mu\mu}^2\delta_{i1}\delta_{j1}\int_{k'}\int_0^t \mathrm{d}t'\tilde{C}^{\mu\mu}(\mathbf{k}')\tilde{c}_0(-\mathbf{k}',t')\times[1-\tilde{c}_0(\mathbf{k}',t)], \tag{A.25}$$

$$\delta^{\mu\nu}D_{ij}^{\text{eff}}(t) = u^2\sigma_{\mu\mu}^2\sigma_{\nu\nu}^2\int_{k'}\int_0^t \mathrm{d}t'\tilde{C}^{\mu\mu}(\mathbf{k}')[\delta_{i1}\delta_{j1}A(\mathbf{k}',t') + \delta_{j1}A_i(\mathbf{k}',t',0) + \delta_{i1}A_j(\mathbf{k}',t',0) + C_{ij}^{\nu\nu}(t')]\times[\tilde{c}_0(-\mathbf{k}',t') - \tilde{c}_0(-\mathbf{k}',t)\tilde{c}_0(\mathbf{k}',t-t')]. \tag{A.26}$$

We obtain the leading behavior of $\delta^{\mu\nu}u_i^{\text{eff}}(t)$ and $\delta^{\mu\nu}D_{ij}^{\text{eff}}(t)$ for small inverse Peclet numbers, (38) and (39) by inserting the expansions

$$\tilde{c}_0(-\mathbf{k}',t') = \exp(-k_j'^2 l_j^2\epsilon_j t'/\tau_u - \mathrm{i}k_1' l_1 t'/\tau_u) = \exp(-\mathrm{i}k_1' l_1 t'/\tau_u) + \cdots \tag{A.27}$$

and

$$\tilde{c}_0(-\mathbf{k}',t)\tilde{c}_0(\mathbf{k}',t-t') = \exp(-2k_j'^2 l_j^2 t/\tau_{D_j})\tilde{c}_0(\mathbf{k}',-t') = \exp(-2k_j''^2 l_j^2 t/\tau_{D_j} - \mathrm{i}k_1' l_1 t'/\tau_u) + \cdots, \tag{A.28}$$

into (A.23) and (A.26). The dots denote subleading contributions of the order of the inverse Peclet numbers.

References

[1] Chrysikopoulos C, Roberts KPKP. Analysis of one dimensional solute transport through porous media with spatially variable retardation factor. Water Resour Res 1990;26:437–46.

[2] Bellin A, Rinaldo A, Bosma WJP, Zee SEATMVd, Rubin Y. Linear equilibrium adsorbing solute transport in physically and chemically heterogeneous posous formations 1. Analytical solutions. Water Resour Res 1993;29(12):4019–30.

[3] Miralles-Wilhelm F, Gelhar LW. Stochastic analysis of sorption macrokinetics in heterogeneous aquifers. Water Resour Res 1996;32(6):1541–9.

[4] Reichle R, Kinzelbach W. Effective parameters in heterogeneous and homogeneous transport models with kinetic sorption. Water Resour Res 1998;34(4):583–94.

[5] Metzger D, Kinzelbach H, Kinzelbach W. Asymptotic trasnport parameters in a heterogeneous porous medium: comparison of two ensemble-averaging procedures. Stochastic Env Res Risk Assessment 1999;13:396–415.

[6] Metzger D, Kinzelbach H, Kinzelbach W. Effective dispersion of a solute cloud in a chemically heterogeneous porous medium: comparison of two ensemble-averaging procedures. Water Resour Res 1996;32(11):3311–9.

[7] Attinger S, Dentz M, Kinzelbach H, Kinzelbach W. Temporal behaviour of a solute cloud in a chemically heterogeneous porous medium. J Fluid Mech 1999;386:77–104.

[8] Dentz M, Kinzelbach H, Attinger S, Kinzelbach W. Temporal behavior of a solute cloud in a heterogeneous porous medium: 1. Point-like injection. Water Resour Res 2000;36(12):3591–604.

[9] Dentz M, Kinzelbach H, Attinger S, Kinzelbach W. Temporal behavior of a solute cloud in a heterogeneous porous medium: 2. Spatially extended injection. Water Resour Res 2000;36(12):3605–14.

[10] Silliman SE, Simpson ES. Laboratory evidence of the scale effect in dispersion of solutes in porous media. Water Resour Res 1987;23:1667–73.

[11] Burr D, Naff R. Nonreactive and reactive solute transport in three-dimensional heterogeneous porous media: mean displacement, plume spreading, and uncertainty. Water Resour Res 1994;30(3):791–815.

[12] Cortis A, Berkowitz B. Anomalous transport in "classical" soil and sand columns. Soil Sci Soc Am J 2004;68:1539–48.

[13] Fernández-Garcia D, Illangasekare TH, Rajaram H. Differences in the scale dependence of dispersivity and retardation factors estimated from forced-gradient and uniform flow tracer tests in three-dimensional physically and chemically heterogeneous porous media. Water Resour Res 2005;41(W03012). doi:10.1029/2004WR003125.

[14] Fernández-Garcia D, Rajaram H, Illangasekare TH. Assessment of the predictive capabilities of stochastic theories in a three-dimensional laboratory test aquifer: effective hydraulic conductivity and temporal moments of breakthrough curves. Water Resour Res 2005;41(W04002). doi:10.1029/2004WR003523.

[15] Lichtner PC, Tartakovsky DM. Upscaled effective rate constant for heterogeneous reactions. Stochastic Environ Res Risk Assessment (SERRA) 2003;17(6):419–29.

[16] Aucour AM, Tao FX, Moreira-Turcq P, Seyler P, Sheppard S, Benedetti MF. The Amazon River: behaviour of metals (Fe, Al, Mn) and dissolved organic matter in the initial mixing at the Rio Negro/Solimoes confluence. Chem Geol 2003;197(1-4):271–85.

[17] Tonkin J, Balistrieri L, Murray J. Modeling metal removal onto natural particles formed during mixing of acid rock drainage with ambient surface water. Env Sci Tech 2002;36(3):484–92.

[18] Sanford W, Konikow L. Simulation of calcite dissolution and porosity changes in saltwater mixing zones in coastal aquifers. Water Resour Res 1989;25:655–67.

[19] Abarca E, Carrera J, Sanchez-Via X, Dentz M. Anisotropic dispersive henry problem. Adv Water Resour, in press. doi:10.1016/j.advwatres.2006.08.005.

[20] Chu M, Kitanidis PK, McCarty PL. Modeling microbial reactions at the plume fringe subject to transverse mixing in porous media: when can the rates of microbial reaction be assumed to be instantaneous? Water Resour Res 2005;41:WR003495.

[21] Knutson CE, Werth CJ, Valocchi AJ. Pore-scale simulation of biomass growth along the transverse mixing zone of a model two-dimensional porous medium. Water Resour Res 2005;41:W07007.

[22] De Simoni M, Carrera J, Sanchez-Vila X, Guadagnini A. A procedure for the solution of multicomponent reactive transport problems. Water Resour Res 2005;41:WR004056.
[23] Kinzelbach W, Ackerer P. Modlisation du transport de contaminant dans un champ d'coulement non-permanent. Hydrolgologie 1986;2:197–205.
[24] Rehfeldt K, Gelhar L. Stochastic analysis of dispersion in usteady flow in heterogeneous aquifers. Water Resour Res 1992;28(8): 2085–99.
[25] Kabala Z, Sposito G. A stochastic model of reactive solute transport with time-varying velocity in a heterogeneous aquifer. Water Resour Res 1991;27(3):341–50.
[26] Zhang D, Neuman SP. Head and velocity covariances under quasi-steady state flow and their effects on advective transport. Water Resour Res 1996;32:77–83.
[27] Dagan G, Bellin A, Rubin Y. Lagrangian analysis of transport in heterogeneous formations under transient flow conditions. Water Resour Res 1996;32(4):891–9.
[28] Cirpka OA. Effects of sorption on transverse mixing in transient flows. J Cont Hydrol 2005;78:207–29.
[29] Dentz M, Carrera J. Effective dispersion in temporally fluctuating flow through a heterogeneous medium. Phys Rev E 2003;68:036310.
[30] Cirpka OA, Attinger S. Effective dispersion in heterogeneous media under random transient flow conditions. Water Resour Res 2003;39(9):1257.
[31] Dentz M, Carrera J. Effective solute transport in temporally fluctuating flow through heterogeneous media. Water Resour Res 2005;41:W08414.
[32] Kitanidis PK. Prediction by the method of moments of transport in a heterogeneous formation. J Hydrology 1988;102:453–73.
[33] Kitanidis PK. The concept of the dilution index. Water Resour Res 1994;30:2011.
[34] Cirpka OA. Choice of dispersion coefficients in reactive transport calculations on smoothed fields. J Cont Hydrol 2002;58:261–82.
[35] Cirpka OA, Frind E, Helming R. Numerical simulation of biodegradiaton controlled by transverse mixing. J Cont Hydrol 1999;40(2):159–82.
[36] Abramowitz M, Stegun IA. Handbook of mathematical functions. New York: Dover Publications; 1972.
[37] Taylor GI. Dispersion of soluble matter in solvent flowing through a tube. Proc Roy Soc A 1953;219:186–203.
[38] Tartakovsky DM, Lichtner PC, Pawar RJ. PDF methods for reactive transport in porous media. Kovar K, Hrkal Z (editors), Conference on calibration and reliability in groundwater modelling (ModelCARE 2002), Prague, Czech Republic, June 17–20, IAHS-AISH Publication No. 277; 2003. p. 162–7.
[39] Matheron G, Marsily Gd. Is transport in porous media always diffusive? A counter-example. Water Resour Res 1980;16:901–17.
[40] Clincy M, Kinzelbach H. Stratified disordered media: exact solutions for transport parameters and their self-averaging properties. J Phys A 2001;34:7141–52.